Research Square

Preprints are preliminary reports that have not undergone peer review.
They should not be considered conclusive, used to inform clinical practice,
or referenced by the media as validated information.

Serological Proteome Analysis (SERPA) Reveals Breast Cancer-Associated Autoantibodies Targeting Placental Antigens

Sara Khoramisarvestani
khoramisara@gmail.com
Avicenna Research Institute https://orcid.org/0000-0002-0534-5345
Sorour Shojaeian
Alborz University of Medical Sciences
Kambiz Gilany
Avicenna Research Institute
Negar Vanaki
Tehran University of Medical Sciences
Abbas Ghaderi
Shiraz University of Medical Sciences Shiraz Institute for Cancer Research
Mohammad-Hossein Ghahremani
Tehran University of Medical Sciences
Faezeh Sabzehei
Avicenna Research Institute
Jacob Skallerup Andersen
Aalborg University: Aalborg Universitet
Milad Sadeghzadeh
Tehran University of Medical Sciences
Hengameh Ahmadi
Avicenna Research Institute
Haleh Soltanghoraee
Avicenna Research Institute
Fazel Shokri
Tehran University of Medical Sciences
Mohammad-Mehdi Amiri
Tehran University of Medical Sciences
Asiie Olfatbakhsh
ACECR: Academic Center for Education Culture and Research
Ramin Sarrami-Forooshani
ACECR: Academic Center for Education Culture and Research
Allan Stensballe
Aalborg University: Aalborg Universitet
Mahmood Jeddi-Tehrani
Avicenna Research Institute
Amir-Hassan Zarnani
Avicenna Research Institute https://orcid.org/0000-0003-4503-299X

Research Article

Keywords: Autoantibody, breast cancer, placental proteins, biomarker, early diagnosis

Posted Date: August 6th, 2026

DOI: https://doi.org/10.21203/rs.3.rs-10289101/v1

License: This work is licensed under a Creative Commons Attribution 4.0 International License. Read Full License

Abstract

Background

The association between placental development and cancer formation was first proposed over a hundred years ago. In our current investigation, we pioneered the application of serological proteome analysis (SERPA) of human placental proteins to detect tumor-associated antigens that trigger autoimmune responses in breast cancer patients.

Methods

We employed SERPA to examine serum reactivity against first-trimester placental (FTP) proteins in 86 early-stage breast cancer (BrC) patients and 86 non-cancer controls (non-BrC). Following initial screening, we isolated and characterized differentially reactive proteins using LC-MS tandem mass spectrometry. From these, we unambiguously identified 12 placental proteins showing the most pronounced differential expression between patient and control groups. These candidate biomarkers underwent rigorous validation through both ELISA and immunohistochemical (IHC) analyses.

Results

Our SERPA screening revealed thirty-three placental proteins exhibiting differential immunoreactivity with breast cancer-associated autoantibodies. Subsequent validation of twelve candidates identified six proteins including PDIA3 ($p = 0.0059$), STIP1 ($p = 0.027$), CCT2 ($p = 0.0025$), PARK7 ($p = 0.0002$), PRDX6 ($p = 0.016$) and LDHB ($p = 0.0083$) that showed statistically significant elevated reactivity with BrC patient sera. Gene Ontology analysis demonstrated that these autoantibody-targeted placental proteins primarily participate in immune regulation and cellular stress response pathways. Immunohistochemistry (IHC) staining of placenta using antibodies directed against PARK7 and PRDX6 recombinant proteins (cloned from FTP), localized their expression predominantly to placental cytotrophoblasts. Notably, in IHC staining of breast cancer and normal breast tissues, PARK7 and PRDX6 exhibited distinct subcellular localization patterns, significantly stronger nuclear staining in normal tissues ($p < 0.001$) versus predominant cytoplasmic localization in malignant specimens ($p < 0.0001$). Serum immunoreactivity from BrC patients displayed remarkable specificity, targeting nuclear and cytoplasmic compartments of rare cytotrophoblast subpopulations and syncytial nuclear aggregates. Through combinatorial analysis of placental-reactive autoantibodies, we identified a set of promising biomarker panels with specificity and sensitivity ranging from 64–73% and 77–97%, respectively, demonstrating potential for non-invasive breast cancer detection.

Conclusion

To the best of our knowledge, this study is the first to propose the use of placental proteins for early breast cancer screening. Our findings establish a novel approach for breast cancer detection and identify potential targets for immunotherapy. However, further refinement and clinical adaptation are needed before translation into diagnostic or therapeutic applications.

Introduction

The idea that there are evolutionary parallels between cancer cells and the placental trophoblasts stems from a theory put forward by the Scottish embryologist John Beard. He proposed cancer as ectopic trophoblastic cells (1, 2). Although they differ in their physiological settings and evolutionary backgrounds, the processes of placentation and carcinogenesis share numerous similarities, which can generally be grouped into four categories: metabolic and cellular behavior, protein expression and molecular markers, signaling pathways, and the tissue microenvironment (2). Invasive placentation and cancer metastasis both entail the elaborate migration and infiltration of cells into neighboring tissues, coupled with the formation of new blood vessels to sustain their expansion. The sophisticated interactions of molecules that govern cellular activity—such as growth factors, cytokines, and extracellular matrix components—are pivotal in each of these processes. In both scenarios, cells must evade local immune defenses, trigger invasive mechanisms, and stimulate angiogenesis (3). Based on the aforementioned similarities between carcinogenesis and placentation, it could be inferred that the placenta can be considered a physiological tumor. Within this framework, the presence of placenta-specific antigens in various cancers has led researchers to explore these molecules as potential targets for anticancer treatments (2).

Both cancer cells and trophoblasts produce a substantial array of tumor-associated antigens, making them potential targets for cancer screening and early diagnosis (4). Because screening tests are generally administered to asymptomatic individuals, an optimal screening method should be noninvasive, cost-effective, and sufficiently reliable for large-scale population use (5, 6). Despite this, current immunodiagnostic approaches in routine screening and clinical diagnostics primarily focus on measuring a few tumor markers in serum including CA125 in ovarian cancers, CEA in gastrointestinal malignancies, and PSA in prostate cancers (7).

The detection of cancer-associated autoantibodies (cAAbs) represents a highly promising approach for cancer screening. cAAbs serve as highly sensitive biosensors capable of detecting disease-related alterations long before clinical symptoms appear. The focus on cAAbs for early cancer detection stems from their biological amplification, early response, and remarkable stability, offering a potential solution to the challenge of biological heterogeneity in cancer biomarker research (8, 9). While clinically validated autoantibody markers for early cancer screening have not yet been established, significant advancements have occurred in developing methodologies to identify and verify potential autoantibody signatures. Technologies for discovery and validation using autoantibody profiles are now maturing being based on ELISA and protein array-based approache .(10) Numerous studies have employed diverse techniques

to detect cAAbs across various cancer types, including breast (11), colorectal (12), lung (13), ovarian (14), and gastrointestinal cancers (15). Each of these methods presents distinct strengths and limitations in terms of comprehensively identifying antigenic epitopes.

Research on cancer screening using cAAbs often employs lysates derived from tissues or cell lines as antigen sources (16, 17). Nevertheless, this methodology may lack complete reliability because of the inherent heterogeneity of tumor tissues and potential modifications in the molecular profile of cultured cancer cell lines that can arise during in vitro propagation. Consequently, antigens identified from these sources may not be fully representative of those found in native cancer cells (18, 19). In our previous work, we reported that the first-trimester placenta (FTP) proteome contains a greater number of cancer-related antigens than the term placenta (20). Furthermore, supporting the antagonistic pleiotropy theory of cancer and placental evolution, which suggests that metastatic cancer is a negative consequence of invasive placentation (21), we recently identified stage-specific autoantibodies targeting FTP antigens in multiple malignancies, including breast cancer (BrC) (22). In this study, we aim to extend our previous findings to address a vital inquiry regarding the identification of placental proteins that trigger the production of cAAbs in BrC by utilizing the serological proteome analysis (SERPA) technique.

Methods

The project consisted of three major phases to identify (discovery and development phases) and validate (validation phase) new placenta-reactive autoantibodies in sera of women with breast cancer. The detailed flowchart of the study is shown in Fig. 1.

This study was approved by the Avicenna Research Institute (ARI) Ethics and Review Boards (Ethical Approval No. 1397.007). All procedures were conducted in accordance with the Declaration of Helsinki. Before sampling, all participants provided written informed consent.

Sample collection and processing

During the discovery phase, placental samples were collected from four pregnant women (gestational age 10 ± 2 weeks) after volunteer termination of pregnancy and four term placenta (gestational age 38 ± 1 week) after caesarian delivery. We reported earlier, using 2-dimensional gel electrophoresis (2DE) followed by liquid chromatography-tandem mass spectrometry (LC-MS), that first-trimester placenta (FTP), compared to term placenta (TP), differentially express more proteins involved in different aspects of carcinogenesis (20). Consequently, we observed that patients with cancer produce detectable levels of placenta-reactive AAbs. This was extremely the case for BrC patients, in which patients with early-stage disease produced AAbs reactive with the FTP (22). Accordingly, we selected FTP as the source of antigens for our subsequent investigations. To extract the proteins, 0.1 gram of the pulverized sample was homogenized in 1 mL of lysis buffer containing 8 M urea, 2% CHAPS, and 2% dithiothreitol (DTT) in 5 mM Tris-HCl pH 7.6. The mixture was then incubated for 15 min on ice with intermittent gentle vortexing followed by centrifugation of the homogenates at 15,000× g for 1 h at 4°C. Supernatants were then collected and their protein content was measured by a 2-D Quant Kit (GE Healthcare, Chicago, IL, USA).

Serum samples were collected from women who were referred for to the Motamed Breast Cancer Institute (MCI) for routine breast cancer screening program without having suspicious sign or symptoms. Patients who had fine-needle aspiration (FNA) pathology results, were divided into two groups: newly diagnosed patients in stage 1 or 2 breast cancer and non-breast cancer patients who had benign breast masses. Patients with missed clinical information and pathologic results were excluded from the study. Serum samples were collected from 86 breast cancer and 86 age-matched non-breast cancer women and stored at -70º C. None of the subjects had a previous history of autoimmune disorders, chronic inflammatory diseases, cancer and related treatments, immunosuppressive drug intake, or pregnancy within at least three months before sampling. Detailed information on sample demographic data is available in our recent publication (22).

To visualize the localization of the selected placental biomarkers, breast cancer, normal breast, and FTP tissues were collected. Tissue fragments from 24 early-stage breast cancer cases and 9 non-breast cancer patients were collected and processed for formalin fixed paraffin-embedded immunohistochemistry (IHC). Additionally, tissue fragments from 2 FTP were processed in parallel as above.

Two-Dimensional Gel Electrophoresis

In the first dimension, 100 µg protein extracted from FTP tissues was mixed with 125 µl of rehydration buffer and applied to an immobilized pH gradient (IPG) strip (7 cm, pH 5–8) (Bio-Rad, Hercules, CA, USA). A total of 12 IPG strips were rehydrated and used in this study. Each set of three strips was run in parallel under identical conditions. Isoelectric focusing (IEF) was performed at 4000 V for 120 min, followed by 10000 Vh, and an additional 150 Vh. The strips were then immediately stored at -80°C overnight and subsequently used for second-dimension gel electrophoresis with 8–15% precast gradient gels (Bio-Rad). One 2-DE gel was stained using Coomassie colloidal brilliant blue (CCB) dye, while the other two SDS-PAGE gels were used for Western blotting using pooled sera from breast cancer and non-breast cancer patients. This procedure was repeated three more times to produce four replicates for each setting.

Western Blot: For identification of placental antigens reactive with serum AAbs, the whole FTP proteome was separated in 8–15% SDS-polyacrylamide gels and then transferred to polyvinylidene difluoride (PVDF) membranes (Sigma) at 100 V for western blot analysis. Then, the membranes were blocked with 3% bovine serum albumin (BSA, Sigma) prepared in PBS and 0.1% Tween 20 (PBST) and individually were incubated with pool sera prepared from either 86 BrC or 86 non-BrC sera diluted 1:750 in 5% skim milk (Merck) PBST solution. Horseradish peroxidase (HRP)-conjugated rabbit anti-human Ig (Sina Biotech, Iran) was used as secondary antibody at 1:20,000 dilution. Finally, the immunoreactive dots were detected with Select enhanced chemiluminescence (ECL) kit (GE Healthcare, Sweden). Membranes from breast cancer and non-breast cancer patients were imaged and photographed simultaneously (Vilber Lourmat, Fusion FX) to prevent interfering factors affecting signal intensity.

Post staining image analysis and spot picking

After Western blot and ECL development, the PVDF membranes were stained using Coomassie blue (CB) 0.1% for 4 min at room temperature (RT) and excess dye was removed by washing twice for an hour. The membrane was dried at RT and gels were imaged using Fusion FX Imager (Vilber, USA). PVDF and Gel alignment was a critical step due to master gel size change throughout the staining process. Photos of Coomassie blue-stained PVDF membranes were aligned with those of ECL stained membranes and all ECL signal spots were flagged on CB-stained PVDF membranes. Then the flagged spots were aligned with the master gel image by photoshop software (Adobe CS6). Moreover, to identify reproducible and differential spot signals in four patient and four control membranes, images were matched using inter-class and intra-class comparison using Image Master 2D software (GE Healthcare Platinum v 6.0). The density of each spot in the patient and control groups was scored by 4 independent observers. This approach resulted in a highly accurate representation of the protein analysis, and robust the reliability of mapping step. The flagged spots that showed distinguished reactivity between patient and normal groups were selected, and characterized using ImageJ software (Ras band, W.S. Mac OS X) and punched from the master gels using a disposable biopsy puncher (1mm Kai Medical, India) for protein identification.

Gel based mass spectrometry- protein identification: Spots that were either present in only one of the case or control gels or showed statistically significant differential expression (fold change > 1.5) between case and control were selected for identification by the EvoSepOne (Evosep, Odense, Denmark)-timsTOF™ Pro2 LC-MS (Bruker, Bremen, Germany) system. Excised protein spots were prepared for LC-MS based identification essentially according to (PMID: 32087365). Protein spots were de-stained by acetonitritrile (AcN, Sigma-Alrich)-100mM Ammoniumbicarbonate (Ambic, Sigma-Aldrich) incubation steps (10min) at 0%, 50% and 100%AcN. At 100% AcN the gel plugs were dehydrated and remaining AcN evaporated by vacuum centrifugation. In-gel reduction and alkylation were performed at 10mM TCEP and 25 mM chloroacetic acid (Sigma-Aldrich, CAA) for 30min at 56°C followed washing step with dehydration by 50% and 100% AcN incubations. The shrinked gel-plugs were swelled in trypsin digestion buffer (0.5 ug in 50 mM Ammoniumbicarbonate) and incubated O/N at 37°C. Peptides were extracted and peptide concentration measured by fluorescent quantitative peptide assays (Pierce). A total of 500 ng peptide was loaded on Evotips according to manufacturer's recommendations and analyzed by LC-MS using Evosep One (Evosep, Odense, Denmark) interfaced to a timsTOF PRO2 (Bruker, Bremen, Germany) using a 100 SPD method and standard nESI-DDA-PASEF in positive ion mode. Protein identifications were accomplished by database searching against a human reference proteome database (UP000005640_9606; 20.460 proteins; NOV2022) using Maxquant (v. 2.0.3.0) with default settings and fixed modifications (carbamitomethyl_Cys) and variable (oxidized_Met). Protein identifications were filtered and sorted according to number of peptides associated to the protein sequence, sequence coverage, theoretical pI and molecular weight in comparison to experimentally obtained pI for the analyzed gel-spot. The mass spectrometry proteomics data have been deposited to the ProteomeXchange Consortium(23) via the PRIDE partner repository with the dataset identifier PXD071458.

Validation of breast cancer-associated autoantibodies binding to identified placental proteins: Twelve high score selected proteins were purchased from MyBiosource (Austria). These proteins were diluted in coating buffer (PBS, pH 7.0) to a final concentration of 1 µg/mL and subsequently coated onto 96-well microtiter plates (SPL Life Science, Korea) at room temperature (RT) for 120 min. This was followed by four washes with PBS-Tween 20 (PBST; pH 7.4; 0.05% Tween), each for 1 min. The plates were then blocked using 5% skim milk diluted in PBST at 37°C for 90 min, followed by another four washes with PBST. Subsequently, sera samples from case and control groups were individually diluted 1:100. The diluted sera were added to the antigen-coated wells and incubated 1h at RT. After incubation, the plates were washed three times with PBST. Ready-to-use HRP-conjugated goat anti-human IgG (Diazist, Tehran, Iran) was added and incubated for 45 min at RT followed by addition of TMB substrate (Arya Pishtaz Novin, Tehran, Iran). Optical density (OD) was measured within 10 min at 450 nm, with a reference OD at 620 nm, using a Biochrom ELISA plate reader (Anthos 2020).

Production and characterization of recombinant proteins:To ensure the recombinant proteins closely matched their placental counterparts, human FTP was used to extract mRNA, followed by cloning and recombinant protein expression. The coding sequences (CDS) of the PARK7 (NM_007262.5) and PRDX6 (NM_004905.3) genes were obtained from the NCBI Nucleotide database (https://www.ncbi.nlm.nih.gov/nucleotide/). For the restriction cloning, primers with overhangs of specific restriction sites (EcoRI and HindIII for PARK7 and EcoRI and XhoI for PRDX6) and enzyme placement were used. (PARK7 forward primer: 5′ CCGGAATTCATGGCTTCCAAAAG 3′, PARK7 reverse primer: 5′CCCAAGCTTCTAGTCTTTAAGAAC 3′. PRDX6 forward primer: 5′ CCGGAATTCATGCCCGGAGGTCTG 3′, PRDX6 reverse primer: 5′CCGCTCGAGTTAAGGCTGGGGTGTG 3′). The RNA was isolated using REX solution (Pishgam Biotech Co., Iran) from human FTP tissue. cDNA was synthesized according to the manufacturer's protocol (Pishgam Biotech Co., Iran) and used as a PCR template. PARK7 and PRDX6 amplification was performed during the initial denaturation step at 95°C for 5 min, followed by 40 cycles of denaturation at 95°C for 45 seconds, annealing at 57°C for 45 seconds, and extension at 72°C for 45 seconds. A final extension step was performed at 72°C for 5 min. The PCR products were purified using a FavorPrep™ Gel/PCR Purification Kit (FAVORGEN BIOTECH CORP., Taiwan).

The double digestion reaction of the pET-28a(+) vector and purified inserts was performed by incubating the mixture for 4h at 37°C. Then, the reaction was heat-inactivated at 65°C for 20 min. The digested vector and inserts were incubated with T4 DNA ligase (BIO BASIC, Canada) overnight at 16°C. The ligation reaction was set up at a 1:7 M ratio of 50 ng of vector to insert in a total volume of 10 µl. The ligation products were transformed into chemically competent (CaCl2 0.1 M) E. coli BL21(DE3), and the recombinant colonies were selected on LB agar containing 50 µg/ml of kanamycin. The recombinant colonies were confirmed by colony PCR using gene specific primers. The recombinant colonies were cultured in LB broth media at 37°C/250 rpm in a shaker incubator. The induction of expression was established using different concentrations (0.2, 0.4, 0.6, and 1 mM) of isopropyl β-d-1-thiogalactopyranoside (IPTG, Bio Basic, Canada). Following 2, 4, 6, and 16 h of induction, bacterial samples were collected, and the expression of the recombinant proteins was examined using 12% SDS-PAGE. Protein purification was performed using Ni affinity chromatography under denaturing conditions (8 M urea) in lysis (5 mM imidazole, 50 mM NaH2PO4, 300 mM NaCl), wash (50 mM imidazole, 50 mM NaH2PO4, 300 mM NaCl), and elution (250 mM imidazole, 50 mM NaH2PO4, 300 mM NaCl) buffers due to inclusion body formation. Protein concentration was evaluated using the Bradford assay. Purified proteins were identified by Western blot analysis. In brief, the induced bacterial lysate was applied to a 12% SDS-PAGE gel and transferred to a polyvinylidene fluoride (PVDF) membrane. The membrane was blocked with 5% skimmed milk at room temperature for two h, followed by five washes with TBST buffer (Tris-buffered saline with 1% Tween 20). The membrane was then soaked in 1:20,000 HRP-conjugated anti-His-tag antibody (Thermo Fisher Scientific - USA) at 4°C overnight. After five washes with TBST, the membrane was incubated with a 3,3'-diamino-benzidine (DAB)/H_2O_2 substrate (Sigma-Aldrich, USA) at room temperature. Once the protein bands were visible, the membrane was washed with distilled water.

Polyclonal antibody production: Two New Zealand white rabbits (age: 12 weeks) were immunized five times, with a three-week interval for the first and second injections and two-week intervals for the subsequent injections. Rabbits were immunized with placental-derived peroxiredoxin 6 (PRDX6), or Parkinsonism-associated deglycase (PARK7) recombinant protein. For the initial immunization, 50 µg recombinant protein diluted in phosphate-buffered saline (PBS) (total volume = 500 µl) were mixed with an equal volume of Freund's complete adjuvant (Sigma) and injected subcutaneously in four regions in the upper thigh and lower back. For the following immunizations, 25 µg protein was injected in the same way using and Freund's incomplete adjuvant (Sigma). Blood samples were drawn by venipuncture before each immunization and 7 days after the last immunization. The blood was allowed to clot for 2 to 3 h at room temperature before serum preparation. Subsequently, the titration of the polyclonal antibodies was performed using ELISA test.

Localization of placental antigen in breast cancer tissue: To validate the ELISA results and visualize the localization of placental antigens, immunohistochemical (IHC) staining was performed on breast and placental tissues. Tissue fragments from the central zone of 24 early-stage breast cancer (Invasive Ductal Carcinoma) specimens and 9 normal breast tissues (collected from mastoplasty cases) and 2 normal FTP tissues were embedded in paraffin blocks for tissue array IHC. Tissue sections, 3 µm thick, were prepared for analysis. The slides underwent deparaffinization in xylene (Sigma Aldrich, Oakville, Canada) and were subsequently rehydrated in graded ethanol. Following this, the tissue sections were subjected to heat-induced antigen retrieval in 0.1M Citrate buffer (pH 6) at 95°C. To block endogenous peroxidase activity, the sections were immersed in 1% H_2O_2 for 15 min. After blocking by 5% sheep serum in 30 min, the slides were incubated with specific polyclonal antibodies against placenta-derived recombinant proteins (PARK7, PRDX6). Optimal results were achieved with a 1:100 dilution of sera with a 30 min incubation at 4°C. After washing, poly-HRP-detection system (BioVision, SinaBiotech, Iran) was applied. Signal visualization was achieved using diaminobenzidine (DAB) for 5 min. The slides were then washed, rehydrated, stained with hematoxylin, and mounted. Negative reagent control slides utilize pre-immunized mice serum. Images were captured using an Olympus BX51 microscope equipped with a DP71 camera. IHC scoring was done according the protocol published previously(24).

Assessment of reactivity of breast cancer-associated autoantibodies with human FTP:To visualize the localization of the placental antigens reacting with breast cancer-associated autoantibodies, human on human immunohistochemistry was performed on human FTP as we described elsewhere (22). In brief, after deparaffinization, rehydration, and heat-induced antigen retrieval, endogenous peroxidase was blocked. Pooled sera from early-stage breast cancer patients and non-breast cancer non-pregnant females were used as primary antibodies, with optimized conditions (overnight incubation at 4°C, 1:20 dilution, followed by HRP detection). Signal visualization used DAB, with hematoxylin counterstaining. Controls included serum-free (negative) and FTP-immunized rabbit serum (positive) probed with a poly-HRP detection system.

Bioinformatics analysis

Proteomic data was analyzed to identify optimal combinations for biomarker discovery. Receiver Operating Characteristic (ROC) curves were generated to evaluate the diagnostic performance of individual and combined biomarkers. A combinatorial analysis was performed to assess the sensitivity and specificity of biomarker combinations, visualized through ROC curves and bubble plots implemented in R (version 4.3.2). Bubble plots were used to represent the performance metrics of gold biomarker combinations, with bubble size and color indicating classification accuracy and combination size, respectively.

Pathway enrichment analysis was performed using the clusterProfiler package (version 4.9.3) to identify overrepresented biological pathways based on the Kyoto Encyclopedia of Genes and Genomes (KEGG), Reactome, wikipathways, Panther and Gene Ontology (GO) databases. Enriched pathways with an adjusted p-value < 0.05 were visualized using a Sankey dot plot, generated in R, to illustrate the relationships between differentially expressed proteins and enriched pathways.

Statistical Analysis

Statistical analyses were conducted using SPSS software version 26. Graphs were generated using GraphPad Prism version 9.4.0. Statistical significance was defined as $p < 0.05$. Comparisons between two groups were done with t test. Additionally, using R software to study receiver operating characteristic (ROC) curves, the power, sensitivity, and specificity of each candidate placental protein and placental protein panels were determined.

Results

Patients with breast cancer developed autoantibodies directed against placental proteins: In the current study, we used a SERPA approach for detection of autoantibodies in sera of patients with breast cancer. For this purpose, the pool proteins from four FTP were separated by 2-DE, transferred onto PVDF membranes and incubated with pooled sera from BrC patients or non-breast cancer controls as the primary antibody. Supplementary Fig.1 displays a comparison of SERPA profiles of case and control groups and related stained PVDF and master gel stained with CB. The test was repeated three times and spots with differential reactivity (more than 1.5-fold changes), and reproducible signals were selected and punched for LC–MS/MS analysis. Our SERPA screening revealed thirty-three placental proteins exhibiting differential immunoreactivity with breast cancer-associated autoantibodies. Table I lists placental proteins with differential reactivity with sera from BrC and non-BrC patients.

Table I. placental proteins with differential reactivity with sera from Brc and non-BrC

Protein No.	Experimental MW (kDa)	Experimental PI	IBAQ[1]	Unique peptides[2]	Theoretical MW (kDa)	Z-Score[3]	Sequence coverage
1	120-130	5.5	1411300	72	61.054	323.31	81.5
2	72-82	5	2666400	52	92.468	323.31	39.9
3	65-72	5.5-6	125880	15	37.375	226.94	54.4
4	65-72	5.5-6	34281	19	37.54	143.14	27.9
5	36-46	6-6.5	1628800	26	25.035	323.31	84.8
6	36-46	6-6.5	3995200	17	27.692	323.31	67.2
7	36-46	7	4078800	17	26.076	323.31	57.3
8	95-105	6.5-7	33650	14	54.858	99.504	35
9	95-105	7	147100	39	56.782	323.31	63.2
10	95-105	7-7.5	3532600	39	47.168	323.31	76.5
11	95-105	7.5-8	45450	28	61.397	247.79	55.6
12	130-160	7	42515	22	72.691	295.87	48.3
13	130-160	7-7.5	395420	37	66.193	323.31	75.4
14	130-140	5-5.5	274080	57	70.897	323.31	57
15	130-140	5.5	46755	62	75.872	323.31	54.1
16	130-140	5.5-6	298990	29	51.676	323.31	58
17	30-35	6.5-7	1560000	24	19.891	323.31	89.9
18	105-115	6.5-7	100110	23	52.39	266.37	52.3
19	105-115	6.5-7	528310	40	57.488	323.31	78.9
20	125-135	7.4-7.6	49931	36	64.615	323.31	62.2
21	125-135	7.4-7.6	752900	54	62.639	323.31	63.9
22	75-85	6.5-7	448490	49	50.663	323.31	73
23	72-85	5.5-6	128690	33	46.971	323.31	45.1
24	72-85	5.5-6	828520	1	42.019	323.31	73.5
25	72-85	5.5-6	1.6E+07	1	41.736	323.31	85.3
26	85-105	5.5-6	13837	20	48.121	323.31	21.6
27	85-105	5.5-6	454210	0	50.151	323.31	36.6
28	85-105	5.5-6	25393	22	51.156	323.31	52.7
29	110-120	6.5-7	26395	27	70.389	291.24	36.6
30	40-50	7.3-7.8	877610	19	28.804	323.31	70.5
31	40-50	7.3-7.8	35944	15	28.87	304.75	41
32	40-50	7.3-7.8	117180	24	26.669	323.31	85.1
33	55-65	6-6.5	149520	19	36.638	323.31	55.4

[1] Intensity-Based Absolute Quantification: The intensity of peptides is divided by the number of observable peptides for a specific protein

[2] Unique Peptide: A specific peptide, regardless of its length, found exclusively in a specific protein of interest from the targeted proteome.

[3] Quality of Mass Spectrometry Spectrum reported with a maximum score 323.31

[4] Number of Amino Acids in a specific identified peptides sequence

Based on high confidence tandem MS report and review of SERPA results, a total of 12 proteins were selected for validation phase. Fig.2a shows the close-up sections of SERPA reactivity of these proteins in BrC or non-BrC serum samples.

Placental proteins reactive with BrC-AAbs are involved in immune system processes and cellular response to stress: To explore the biological functions of selected proteins that were differentially expressed between BrC and non-BrC samples, we conducted a functional enrichment analysis of SERPA profile

using Gene Ontology (GO) terms. The results were depicted in a Sankey dot plot to highlight the connections between these proteins and the significantly enriched GO terms (Fig.2b). The analysis identified 33 GO terms with significant enrichment (adjusted p-value < 0.05), most of which fell under the Biological Process category. Notably, a large proportion of the proteins were involved in immune system processes (GO:0002376, -log10(P) = 1.419) and cellular response to stress (GO:0033554, -log10(P) = 1.7). Additional enriched terms were mainly associated with angiogenesis, protein folding, cell proliferation, apoptosis, and immune regulation. Among the proteins, PARK7, HSPD1, and HSPA8 showed the highest number of associations with these GO terms.

The majority of the selected proteins were validated in the confirmatory assay: Selected placental proteins were used as coating antigen in ELISA, and immune reactivity of IgG isotype of sera from 86 breast cancer and 86 non-breast cancer women was separately examined. Among proteins examined, six placental proteins showed significantly higher reactivity with sera from BrC patients including PDIA3 (p=0.0059), STIP1 (p=0.027), CCT2 (p=0.0025), PARK7 (p=0.0002), PRDX6 (p=0.016) and LDHB (p=0.0083) (Fig.3). The reactivity of two other proteins trended toward significance including TPI1 (p=0.07) and HSPA8 (p=0.073), while no statistical significance was observed for other four proteins.

Initial screening of non-cancer control sera (n=96) revealed unexpectedly high immunoreactivity against selected antigens in a subset of samples. To ensure cohort integrity, all controls—defined by a normal breast biopsy at the time of serum collection followed up approximately three years post-sampling. This follow-up identified two individuals who had developed breast cancer and eight with pre-cancerous lesions. These ten samples were subsequently excluded from the final control group (now n=86) prior to final analysis.

Generation and analysis of recombinant PARK7/PRDX6 and their specific antibodies: Colony PCR analysis confirmed successful gene cloning in E. coli BL21 (DE3). The 693bp PRDX6 and 588bp PARK7 PCR products were detected on a 1.5% agarose gel (Fig.4A). Protein purification was performed using Ni-affinity chromatography from recombinant bacteria, and samples of the flow-through, wash, and elution fractions were loaded onto a 12% SDS-PAGE gel. Purified recombinant PARK7 and PRDX6 were identified on the gels (Fig.4B). Purified proteins were loaded on a 12% SDS-PAGE gel, transferred to a PVDF membrane, and then blotted with anti-His tag antibody, after which the desired protein bands of sizes 23.7 kDa and 28.8 kDa for PARK7 and PRDX6, respectively, were detected (Fig.4C). Antibodies were then raised against these placenta-derived PARK7 and PRDX6 proteins, and their binding to the immunizing proteins was confirmed by ELISA. After fourth injection, high titers of anti-PARK7 and anti-PRDX6 antibodies were generated (Fig.4D).

Trophoblasts were main cell population, which expressed PARK7 and PRDX6: To localize placental proteins reactive with BrC-AAbs, we performed Immunohistochemical (IHC) staining of FTP tissues using antibodies against PARK7 and PRDX6. IHC staining with anti-PARK7 revealed distinct reactivity patterns in cytotrophoblasts, primarily localized to the nucleus and cytoplasm, with minimal staining observed in overlying syncytiotrophoblasts (Fig.5). In contrast, PRDX6 was primarily localized to the cytoplasm of syncytiotrophoblasts. Negative control slides treated with pre-immune rabbit sera showed no reactivity.

The expression patterns of PARK7 and PRDX6 differed significantly between breast cancer and normal tissues: Next, the expression of PRDX6 and PARK7 was examined in normal breast tissue and invasive ductal carcinoma (IDC). In normal tissue, both proteins were predominantly nuclear in glandular epithelial cells, with weaker cytoplasmic staining. In contrast, breast cancer tissues exhibited mainly cytoplasmic expression with reduced nuclear reactivity (Fig.6a). Quantitative analysis of staining intensity, localization, percentage of nuclear/cytoplasmic reactivity, and Z-scores (incorporating intensity and percent of positive cells) were performed across ten microscopic fields per sample. Results showed significantly higher nuclear staining intensity for PARK7 in non-cancerous tissues ($p<0.001$) and higher cytoplasmic staining intensity in breast cancer tissues ($p <0.0001$). While the percentage of nuclear staining for PARK7 was similar in both groups, breast cancer tissues had a significantly lower nuclear Z-score ($p < 0.05$) but higher cytoplasmic staining percentage ($p < 0.0001$) and Z-score ($p < 0.0001$). A similar trend was observed for PRDX6 (Fig.6b). No staining was detected in negative controls.

Breast-cancer-associated autoantibodies recognized rare cell population in the human placenta: Immunohistochemical analysis was conducted on FTP using sera from breast cancer (BrC) patients and non-breast cancer (non-BrC) individuals. The BrC sera exhibited a highly specific reactivity pattern with FTP, localized predominantly to a nucleus and cytoplasm of rare subset of cells within the cytotrophoblast layer and syncytial nuclear aggregates (SNA) (Fig.7). Non-BrC samples showed fewer reactive cells.

A set of placental proteins showed promise for sensitive and specific early detection of breast cancer: To evaluate the diagnostic value of the identified placental antigens, a comparison was made between the reactivity of placenta-reactive autoantibodies (AAbs) in BrC patients and non-BrC patients using ROC curves. The area under the curve (AUC) of each placental antigen and antigen combinations were determined. The results of an in-silico analysis of the ROC curves yielded 498 combinations of them 183 combinations had AUC ≥0.7. By focusing on combinations of up to five antigens that had over 60% specificity and 70% sensitivity, 29 promising candidates were identified (Table II). These showed specificity of 64-73% and sensitivity of 77-97% (Supplementary Fig.2), indicating strong potential for a non-invasive breast cancer test.

Table II. specificity and sensitivity of selected placental combination for early diagnosis of breast cancer

Table II. specificity and sensitivity of selected placental combination for early diagnosis of breast cancer

Combination No.	Marker	AUC[5]	SE[6]	SP[7]	ACU[8]	TN[9]	TP[10]	FN[11]	FP[12]	NPV[13]	PPV[14]
790	CCT2-GDI2-HPX-HSPD1-LDHB	0.79	0.965	0.663	0.814	57	83	3	29	0.95	0.741
289	CCT2-GDI2-HPX-LDHB	0.787	0.953	0.663	0.808	57	82	4	29	0.934	0.739
797	CCT2-GDI2-HPX-LDHB-MESDC2	0.787	0.953	0.663	0.808	57	82	4	29	0.934	0.739
870	CCT2-GDI2-LDHB-MESDC2-STIP1	0.786	0.953	0.64	0.797	55	82	4	31	0.932	0.726
801	CCT2-GDI2-HPX-LDHB-STIP1	0.784	0.953	0.663	0.808	57	82	4	29	0.934	0.739
848	CCT2-GDI2-HSPD1-LDHB-PDIA3	0.792	0.942	0.674	0.808	58	81	5	28	0.921	0.743
304	CCT2-GDI2-HSPD1-LDHB	0.79	0.942	0.686	0.814	59	81	5	27	0.922	0.75
311	CCT2-GDI2-LDHB-MESDC2	0.787	0.942	0.663	0.802	57	81	5	29	0.919	0.736
799	CCT2-GDI2-HPX-LDHB-PDIA3	0.784	0.942	0.674	0.808	58	81	5	28	0.921	0.743
70	CCT2-GDI2-LDHB	0.787	0.93	0.674	0.802	58	80	6	28	0.906	0.741
313	CCT2-GDI2-LDHB-PDIA3	0.786	0.93	0.663	0.797	57	80	6	29	0.905	0.734
877	CCT2-GDI2-LDHB-PDIA3-STIP1	0.787	0.919	0.663	0.791	57	79	7	29	0.891	0.731
315	CCT2-GDI2-LDHB-STIP1	0.786	0.919	0.663	0.791	57	79	7	29	0.891	0.731
846	CCT2-GDI2-HSPD1-LDHB-MESDC2	0.789	0.895	0.733	0.814	63	77	9	23	0.875	0.77
850	CCT2-GDI2-HSPD1-LDHB-STIP1	0.789	0.884	0.721	0.802	62	76	10	24	0.861	0.76
851	CCT2-GDI2-HSPD1-LDHB-TPI1	0.8	0.872	0.721	0.797	62	75	11	24	0.849	0.758
76	CCT2-GDI2-TPI1	0.776	0.872	0.616	0.744	53	75	11	33	0.828	0.694
804	CCT2-GDI2-HPX-MESDC2-PDIA3	0.772	0.872	0.64	0.756	55	75	11	31	0.833	0.708
318	CCT2-GDI2-MESDC2-PDIA3	0.772	0.872	0.64	0.756	55	75	11	31	0.833	0.708
316	CCT2-GDI2-LDHB-TPI1	0.789	0.86	0.686	0.773	59	74	12	27	0.831	0.733
878	CCT2-GDI2-LDHB-PDIA3-TPI1	0.788	0.86	0.686	0.773	59	74	12	27	0.831	0.733
813	CCT2-GDI2-HPX-PDIA3-STIP1	0.774	0.86	0.663	0.762	57	74	12	29	0.826	0.718
327	CCT2-GDI2-PDIA3-STIP1	0.774	0.86	0.663	0.762	57	74	12	29	0.826	0.718
862	CCT2-GDI2-HSPD1-PDIA3-STIP1	0.772	0.86	0.651	0.756	56	74	12	30	0.824	0.712
881	CCT2-GDI2-LDHB-STIP1-TPI1	0.788	0.849	0.698	0.773	60	73	13	26	0.822	0.737
887	CCT2-GDI2-MESDC2-PDIA3-STIP1	0.772	0.837	0.674	0.756	58	72	14	28	0.806	0.72
817	CCT2-GDI2-HPX-STIP1-TPI1	0.774	0.814	0.663	0.738	57	70	16	29	0.781	0.707
814	CCT2-GDI2-HPX-PDIA3-TPI1	0.777	0.767	0.733	0.75	63	66	20	23	0.759	0.742

[5] Area under curve
[6] Sensitivity
[7] Specificity
[8] Accuracy
[9] True negative
[10] True positive
[11] False negative
[12] False positive
[13] Negative predictive value
[14] Positive predictive value

Discussion

For over a century, similarities between placental trophoblasts and cancer cells have been recognized, yet only a few placental-derived antigens have been explored for cancer screening so far. Many cancer cells express these placental antigens, which are usually rare in normal adult tissues. These antigens contribute critically to cancer cell growth, invasion, and migration (2).

Breast cancer is a major cause of cancer-related deaths in women, and its incidence rates increased by 0.6%–1% annually between 2015 and 2019, making early diagnosis and preventive screening measures urgent (25). To address this issue, efforts have been made to develop simple, fast, and affordable blood biomarkers for the early detection of breast cancer (26, 27). To be an effective and practical approach, screening tests must meet four basic conditions: 1) must accurately distinguish healthy individuals from those with cancer with high sensitivity and specificity, 2) should detect the disease before the first manifestation of clinical symptoms, 3) should distinguish between aggressive and harmless lesions and 4) should be inexpensive and well-accepted by the target population (28).

One of the most promising approaches for non-invasive cancer diagnosis and screening is the examination of autoantibodies, which can be detected months or even years before the onset of clinical manifestations (29). Tumor-associated antigens may exhibit abnormal structures, altered expression levels, differences in post-translational modifications, or be of retired proteins category, potentially leading to autoantibody production. Due to their stable and well-

characterized structure, autoantibodies have been the focus of numerous cancers screening studies, including breast cancer (30). In cancer screening studies using autoantibodies, cell line lysates or cancer tissue lysates are typically used as the antigen source. However, cell line lysates may not accurately reflect the nature of cancer cells in the human body due to potential changes that occur during cell culture (16–19). Tumors display significant heterogeneity, with diverse molecular features even within the same cancer type (31). Breast cancer, in particular, exhibits substantial molecular and genetic variability, resulting in broad pathological diversity among its subtypes. Notably, tumor antigens can exhibit a passenger phenotype (32), where they are transiently expressed during specific developmental stages but become undetectable in later phases. Consequently, the antigenic signatures observed in cultured cell lines or patient-derived tumor cells may not comprehensively represent the complete antigenic repertoire present in vivo across the broader spectrum of malignant cells. To address these obstacles, the placenta is a suitable source of antigen for tracking cancer-related autoantibodies, given the similarities between placental formation and carcinogenesis.

The complex fetal-maternal interaction during pregnancy involves dynamic molecular and cellular changes, particularly in the placental proteome, to support fetal blood supply (20, 33). A key challenge in this project was assessing how pregnancy stage affects the placental proteome as a source of cancer-associated autoantibodies. We previously compared first-trimester and third-trimester placental proteomes, identifying 120 differentially expressed proteins. Further analysis revealed that cancer-related placental antigens are more abundant in the first trimester (20). To determine whether placental protein reactivity was specific to BrC or observed across other malignancies, we investigated placenta-reactive autoantibodies in sera from patients with breast, gastric, colorectal, and bladder cancers, along with healthy controls. The results demonstrated that cancer patients produced AAbs reactive to FTP proteins regardless of cancer type, with stronger reactivity observed in early-stage BrC (22). These findings supported the hypothesis that placental proteins could facilitate early cancer detection. In the current study, we extended our previous work by identifying the specific placental antigens reactive with BrC-associated autoantibodies and evaluating the diagnostic potential of a 12-protein placental panel for early breast cancer detection. Among the 12 placental proteins identified through SERPA, we validated the reactivity of BrC-associated autoantibodies against PDIA3, STIP1, PARK7, CCT2, PRDX6, and LDHB using ELISA.

PDIA3 regulates cell growth and apoptosis in placental trophoblasts, with higher expression in the first trimester. As an endoplasmic reticulum chaperone, it facilitates protein folding and disulfide bond formation (20). Its overexpression is linked to poor cancer prognosis, making it a potential therapeutic target, since inhibiting PDIA3 slows cancer growth (34–36). Studies associate PDIA3 with multiple cancers, including breast cancer, where its transcript levels may serve as a diagnostic marker (37). Likewise, STIP1 is a endoplasmic reticulum protein with oxidoreductase and chaperone functions, aiding heat shock proteins in DNA synthesis and cell proliferation (38). It acts as an oncoprotein, promoting cancer cell migration and invasion, and serves as a prognostic marker in ovarian (39), esophageal (40), liver (41), and breast cancers (42). Studies in bone cancer suggest its suppression, particularly via the STAT3 pathway, can inhibit cancer cell growth, migration, and invasion (43).CCT2 is a protein from the CCT family, involved in cell morphology regulation and protein folding, assisting ~ 10% of newly synthesized eukaryotic proteins (44). It is important in fetal placental development (45) and is linked to cancer progression. Studies show elevated CCT2 expression in colorectal, gallbladder, liver, and breast cancers, correlating with poor prognosis (46). In colorectal cancer, high CCT2 levels reduce survival (47). In HER2 + breast cancer, CCT2 overexpression worsens prognosis by influencing cell cycle pathways (47). LDHB is a key enzyme in glycolysis, crucial for converting lactate to pyruvate. It plays significant roles in early pregnancy and cancer progression. In early pregnancy, hypoxic trophoblast cells (similar to cancer cells) rely on glycolysis, increasing lactate levels. LDHB helps metabolize lactate, supporting proper placental function and immune regulation (48, 49). It Inhibits apoptosis and stimulates autophagy, aiding tumor progression and facilitates lactate metabolism in the acidic tumor microenvironment, promoting cancer cell survival (50). It is overexpressed in triple-negative breast cancer and higher LDHB levels correlate with poorer clinical outcomes (51).

PARK7 is a multifunctional protein initially linked to Parkinson's disease and its function is to protect cells against oxidative stress and regulate gene translation (52). As an oncoprotein in the RAS signaling pathway, PARK7 promotes cancer progression and influences treatment response (53). PARK7 contributes to peritoneal metastasis in gastric cancer (54). It acts as a deglycase enzyme, and its phosphorylation enhances glycolytic activity, fueling ROS production and Akt pathway activation, sustaining cancer cell proliferation (55). Overexpression of PARK7 in invasive breast cancer has been reported(56). PRDX6 is a mitochondrial peroxidase that regulates oxidative stress responses. PRDX6 counters elevated oxidative stress in cancer cells, supported by transcription factors (NRF2, FOXO) and tumor suppressors (p53) (57). It can bind and reduce phospholipid hydroperoxides and plays an important role in repairing membrane damage caused by oxidative stress. Expression of PRDX6 is elevated in breast, bladder, esophagus, lung, and ovarian cancers (58) and is associated with a more aggressive phenotype in breast cancer (59).

Our enrichment analyses have uncovered additional biological functions for the six proteins studied. PDIA3 was linked to immune system processes, particularly peptide loading onto MHC molecules for antigen presentation. As a component of the antigen processing and presentation machinery (APM), PDIA3 plays a key role in ensuring the correct loading of peptides onto MHC complexes (60). Notably, combining tumor mutational burden with APM components has been proposed to calculate a tumor immunogenicity score, which may serve as a predictive biomarker for cancer immunotherapy responses(61).

GO analysis showed that STIP1 was enriched in pathways related to angiogenesis. While direct evidence connecting STIP1 to angiogenesis is lacking, its interaction with HSP90—a chaperone known to regulate tumor angiogenesis—suggests a potential indirect role (62, 63). PRDX6 showed an association with stress response, which aligns with previously reported findings (64). Interestingly, a new potential link to angiogenesis emerged. Although PRDX1 has been connected to tumor angiogenesis (65), no such association has been previously reported for PRDX6. PARK7 was associated with both lactate metabolism and immune regulation. Recent research highlights the role of lactic acid as a key regulator of immune cell function in the tumor microenvironment (66). PARK7 has been implicated in chaperone-mediated autophagy (CMA), a process known to suppress tumor progression by degrading specific tumor-promoting proteins(67). As a CMA substrate, PARK7 acts as a co-chaperone with R-HSPA5, facilitating the autophagic clearance of misfolded proteins generated by oxidative stress (68), thereby underscoring its protective role against cellular stress.

It is noteworthy that, according to our results, none of the selected antigens per se could be a reliable diagnostic marker for early breast cancer screening, indeed, an overt antibody response against one of the selected antigens was not necessarily associated with the antibody response against other proteins. This finding makes sense because of the great heterogeneity in the molecular mechanisms of breast carcinogenesis, different MHC haplotypes among individuals causing differential immunodominant antibody responses and different time points during breast cancer course, at which sera were collected from experimental group. In this regard, combination ROC analysis could improve the sensitivity while maintaining the maximum possible specificity (69). This approach led to the identification of 29 panels with specificity and sensitivity ranging from 64–73% and 77–97%, respectively.

Nonetheless, where the greatest cost of error is misdiagnosis, optimization of specificity is critical. This is especially true if another test, such as a mammogram in the second step of the clinical workup, can serve to increase specificity. The negative predictive value (NPV) of approximately 76–95% and positive predictive value (PPV) of nearly 75% indicates the suitability of these panels as a screening test and a robust tool for patients with breast lumps.

Although detection of AAbs has been the focus of several stusies for early detection of breast cancer, this report is the first study to employ placenta-reactive AAbs. Using AAbs, different groups have introduced different panels of tumor-associated antigens for detection of breast cancer with sensitivity and specificity of 61–72% and 72–92%, respectively (70–74). However, most of these studies did not report BrC tumor stage. Detection of AAbs for breast cancer diagnosis is justified only when they can be useful before clinical manifestation particularly in the early stages of disease. Indeed, the controls should include - patients with benign type of breast disease, including patients with proliferative and non-proliferative lesions and potential confounding variables including autoimmune disease, hormone therapy, menopausal status, usage of immunosuppressive agents and the number of previous pregnancies should be considered (75). All of these criteria were considered in our study, making the results more reliable.

One important limitation of our study and other reports with the same approach was to use recombinant proteins produced in prokaryotic systems. We showed that, despite a significant elevation of AAbs against PARK7 and PRDX6 in BrC patient sera, these antigens are expressed in breast tissues of BrC and non-BrC women. However, both antigens exhibited different cellular localization in BrC and non-BrC breast tissues. The antigens localized predominantly in the cell nucleus of non-BrC epithelial cells, while BrC cells mainly expressed the antigens in their cytoplasm. This differential compartmentalization could potentially lead to differential post translational modification (PTM) and thereby different pattern of autoantibody production (76). PTMs are crucial regulators of cellular signaling and physiology in healthy and malignant cells. A recent large-scale study analyzing proteogenomic data from 1,110 patients demonstrated widespread alterations in protein acetylation and phosphorylation patterns across 11 cancer types, revealing their involvement in fundamental cancer pathways (77). Moreover, we limited our study to FTP proteome in the isoelectric pH range of 5–8 to maximize the resolution of the proteins in SERPA technique. This might result in neglecting AAbs that react with antigens whose PI falls outside this range.

Conclusion

To our knowledge, this concept of early screening for cancers using placental proteins has not been introduced before. Our results open a new strategy for early diagnosis of breast cancer and finding candidate molecules for targeted immunotherapy of BrC patients. Although our customized placental antigen mini array showed a remarkable performance in non-invasive early diagnosis of breast cancer, further optimization and customization is warranted before it can be used in the clinic. The results of the current study reinforce the link between placental development and carcinogenesis and introduce novel molecular aspects shared between these two phenomena.

Abbreviations

AAb
Autoantibody
2DE
Two-Dimensional Gel Electrophoresis
AUC
Area Under the Curve
BrC
Breast Cancer
CB
Coomassie Blue
CCB
Coomassie Colloidal Brilliant Blue
DAB
3,3'-Diaminobenzidine
DTT
Dithiothreitol
ECL
Enhanced Chemiluminescence
ELISA
Enzyme-Linked Immunosorbent Assay
FNA
Fine-Needle Aspiration
FTP

First-Trimester Placenta
GO
Gene Ontology
HRP
Horseradish Peroxidase
IDC
Invasive Ductal Carcinoma
IEF
Isoelectric Focusing
IHC
Immunohistochemistry
IPG
Immobilized pH Gradient
KEGG
Kyoto Encyclopedia of Genes and Genomes
LC–MS/MS
Liquid Chromatography–Tandem Mass Spectrometry
PBST
Phosphate-Buffered Saline with Tween 20
PCR
Polymerase Chain Reaction
PRIDE
PRoteomics IDEntifications Database
PVDF
Polyvinylidene fluoride
ROC
Receiver Operating Characteristic
RT
Room Temperature
SERPA
Serological Proteome Analysis
SNA
Syncytial Nuclear Aggregates
SDS-PAGE
Sodium Dodecyl Sulfate–Polyacrylamide Gel Electrophoresis
TP
Term Placenta

Declarations

Ethics approval and consent to participate: This study was approved by the Avicenna Research Institute (ARI) Ethics and Review Boards (Ethical Approval No. 1397.007). All procedures were conducted in accordance with the Declaration of Helsinki. Written informed consent was obtained from all participants prior to sample collection.

Consent for publication: Not applicable.

Availability of data and materials: The raw mass spectrometry data reported in this paper have been deposited to the ProteomeXchange Consortium (76) via the PRIDE partner repository with the dataset identifier PXD071458.

Competing interests: The authors declare that they have no competing interests.

Funding: The research reported in this publication was supported by the National Institute for Medical Research Development (NIMAD) (Grant No: 973140), Tehran, Iran, Iran National Science Foundation, (INSF) (Grant No: 542 96013023), Tehran, Iran, and the Avicenna Research Institute (ARI) (grant No: 97016), Tehran, Iran. This work is supported by PLATO by a generous grant from the Danish Agency of Higher Education and Science to establish the PLATO research infrastructure: Danish National Mass Spectrometry Platform for Proteomics and Biomolecular Imaging (grant no. 5229-00012B, www.sdu.dk/PLATO).

Authors' contributions: SKS performed the experiments, analyzed the data, and drafted the manuscript. KG, SSh, AGh, FSh, MMA, and MHG consulted on and verified the analytical methods and critically reviewed the manuscript. FS performed production and characterization of recombinant proteins. NV performed R programming and panel analysis. HA assisted with ELISA setup experiments and production of polyclonal antibodies. MS contributed to manuscript review and prepared the figures and tables. HS provided expert pathological assessment of IHC findings. RSF and AO provided serum and tissue samples and clinical participant data. AS and JSA performed sample preparation, LC–MS analysis, data analysis, and reviewed the manuscript. MJT and AHZ conceived the study, supervised the research, and critically reviewed and finalized the manuscript. All authors read and approved the final manuscript.

Acknowledgements: The authors thank all participants for their contribution to this study. We acknowledge Shiraz University of Medical Sciences and the Motamed Cancer Institute for providing clinical samples, and the Avicenna Research Institute and Aalborg University for technical support.

Authors' information: Not applicable.

References

1. Ross CA. The trophoblast model of cancer. Nutr Cancer. 2015;67(1):61-7.
2. Khorami-Sarvestani S, Vanaki N, Shojaeian S, Zarnani K, Stensballe A, Jeddi-Tehrani M, et al. Placenta: an old organ with new functions. Front Immunol. 2024;15:1385762.
3. Lala PK, Nandi P, Hadi A, Halari C. A crossroad between placental and tumor biology: What have we learnt? Placenta. 2021;116:12-30.
4. Ferretti C, Bruni L, Dangles-Marie V, Pecking AP, Bellet D. Molecular circuits shared by placental and cancer cells, and their implications in the proliferative, invasive and migratory capacities of trophoblasts. Hum Reprod Update. 2007;13(2):121-41.
5. Fitzgerald RC, Antoniou AC, Fruk L, Rosenfeld N. The future of early cancer detection. Nat Med. 2022;28(4):666-77.
6. Chacko N, Ankri R. Non-invasive early-stage cancer detection: current methods and future perspectives. Clin Exp Med. 2024;25(1):17.
7. Laraib U, Sargazi S, Rahdar A, Khatami M, Pandey S. Nanotechnology-based approaches for effective detection of tumor markers: A comprehensive state-of-the-art review. Int J Biol Macromol. 2022;195:356-83.
8. Rauf F, Anderson KS, LaBaer J. Autoantibodies in Early Detection of Breast Cancer. Cancer Epidemiol Biomarkers Prev. 2020;29(12):2475-85.
9. Dudas SP, Chatterjee M, Tainsky MA. Usage of cancer associated autoantibodies in the detection of disease. Cancer Biomark. 2010;6(5-6):257-70.
10. Poulsen TBG, Karamehmedovic A, Aboo C, Jørgensen MM, Yu X, Fang X, et al. Protein array-based companion diagnostics in precision medicine. Expert Rev Mol Diagn. 2020;20(12):1183-98.
11. Yang R, Han Y, Yi W, Long Q. Autoantibodies as biomarkers for breast cancer diagnosis and prognosis. Front Immunol. 2022;13 1035402.
12. Wang H, Li X, Zhou D, Huang J. Autoantibodies as biomarkers for colorectal cancer: A systematic review, meta-analysis, and bioinformatics analysis. Int J Biol Markers. 2019;34(4):334-47.
13. Yang B, Li X, Ren T, Yin Y. Autoantibodies as diagnostic biomarkers for lung cancer: A systematic review. Cell Death Discov. 2019;5:126.
14. Bast RC, Jr., Lu Z, Han CY, Lu KH, Anderson KS, Drescher CW, et al. Biomarkers and Strategies for Early Detection of Ovarian Cancer. Cancer Epidemiol Biomarkers Prev. 2020;29(12):2504-12.
15. Jelski W, Mroczko B. Molecular and Circulating Biomarkers of Gastric Cancer. Int J Mol Sci. 2022;23(14).
16. Klade CS, Voss T, Krystek E, Ahorn H, Zatloukal K, Pummer K, et al. Identification of tumor antigens in renal cell carcinoma by serological proteome analysis. Proteomics. 2001;1(7):890-8.
17. Hamrita B, Chahed K, Kabbage M, Guillier CL, Trimeche M, Chaïeb A, et al. Identification of tumor antigens that elicit a humoral immune response in breast cancer patients' sera by serological proteome analysis (SERPA). Clin Chim Acta. 2008;393(2):95-102.
18. Gillet JP, Varma S, Gottesman MM. The clinical relevance of cancer cell lines. J Natl Cancer Inst. 2013;105(7):452-8.
19. Wilding JL, Bodmer WF. Cancer cell lines for drug discovery and development. Cancer Res. 2014;74(9):2377-84.
20. Khorami Sarvestani S, Shojaeian S, Vanaki N, Ghresi-Fard B, Amini M, Gilany K, et al. Proteome profiling of human placenta reveals developmental stage-dependent alterations in protein signature. Clin Proteomics. 2021;18(1):18.
21. D'Souza AW, Wagner GP. Malignant cancer and invasive placentation: A case for positive pleiotropy between endometrial and malignancy phenotypes. Evol Med Public Health. 2014;2014(1):136-45.
22. Khorami Sarvestani S, Shojaeian S, Sarrami-Forooshani R, Yekaninejad MS, Gilany K, Ghaderi A, et al. Cancer Is Associated with the Emergence of Placenta-Reactive Autoantibodies. Biomedicines. 2023;11(2):316.
23. Perez-Riverol Y, Bandla C, Kundu DJ, Kamatchinathan S, Bai J, Hewapathirana S, et al. The PRIDE database at 20 years: 2025 update. Nucleic Acids Res. 2025;53(D1):D543-d53.
24. Mahmoudi AR, Ghods R, Rakhshan A, Madjd Z, Bolouri MR, Mahmoudian J, et al. Discovery of a potential biomarker for immunotherapy of melanoma: PLAC1 as an emerging target. Immunopharmacol Immunotoxicol. 2020;42(6):604-13.
25. Siegel RL, Giaquinto AN, Jemal A. Cancer statistics, 2024. CA Cancer J Clin. 2024;74(1):12-49.
26. Qiu J, Qian D, Jiang Y, Meng L, Huang L. Circulating tumor biomarkers in early-stage breast cancer: characteristics, detection, and clinical developments. Front Oncol. 2023;13:1288077.
27. Li J, Guan X, Fan Z, Ching LM, Li Y, Wang X, et al. Non-Invasive Biomarkers for Early Detection of Breast Cancer. Cancers (Basel). 2020;12(10):2767.
28. Etzioni R, Urban N, Ramsey S, McIntosh M, Schwartz S, Reid B, et al. The case for early detection. Nat Rev Cancer. 2003;3(4):243-52.
29. Qiu J, Keyser B, Lin Z-T, Wu T. Autoantibodies as potential biomarkers in breast cancer. Biosensors. 2018;8(3):67.
30. Zaenker P, Gray ES, Ziman MR. Autoantibody production in cancer—the humoral immune response toward autologous antigens in cancer patients. Autoimmun Rev. 2016;15(5):477-83.
31. Zhu L, Jiang M, Wang H, Sun H, Zhu J, Zhao W, et al. A narrative review of tumor heterogeneity and challenges to tumor drug therapy. Ann Transl Med. 2021;9(16):1351.
32. McFarland CD, Yaglom JA, Wojtkowiak JW, Scott JG, Morse DL, Sherman MY, et al. The Damaging Effect of Passenger Mutations on Cancer Progression. Cancer Res. 2017;77(18):4763-72.

33. Manna S, Scheel J, Noone A, McElwain CJ, Scaife C, Gupta S, et al. A proteomic profile of the healthy human placenta. Clin Proteomics. 2023;20(1):1.
34. Yang M, Li Q, Yang H, Li Y, Lu L, Wu X, et al. Downregulation of PDIA3 inhibits gastric cancer cell growth through cell cycle regulation. Biomed Pharmacother. 2024;173:116336.
35. Tu Z, Ouyang Q, Long X, Wu L, Li J, Zhu X, et al. Protein Disulfide-Isomerase A3 Is a Robust Prognostic Biomarker for Cancers and Predicts the Immunotherapy Response Effectively. Front Immunol. 2022;13:837512.
36. Paglia G, Minacori M, Meschiari G, Fiorini S, Chichiarelli S, Eufemi M, et al. Protein Disulfide Isomerase A3 (PDIA3): A Pharmacological Target in Glioblastoma? Int J Mol Sci. 2023;24(17):13279.
37. Powell LE, Foster PA. Protein disulphide isomerase inhibition as a potential cancer therapeutic strategy. Cancer Med. 2021;10(8):2812-25.
38. Wang HS, Tsai CL, Chang PY, Chao A, Wu RC, Chen SH, et al. Positive associations between upregulated levels of stress-induced phosphoprotein 1 and matrix metalloproteinase-9 in endometriosis/adenomyosis. PLoS One. 2018;13(1):e0190573.
39. Chao A, Lai CH, Tsai CL, Hsueh S, Hsueh C, Lin CY, et al. Tumor stress-induced phosphoprotein1 (STIP1) as a prognostic biomarker in ovarian cancer. PLoS One. 2013;8(2):e57084.
40. Xu YW, Liu CT, Huang XY, Huang LS, Luo YH, Hong CQ, et al. Serum Autoantibodies against STIP1 as a Potential Biomarker in the Diagnosis of Esophageal Squamous Cell Carcinoma. Dis Markers. 2017;2017:5384091.
41. Chen Z, Xu L, Su T, Ke Z, Peng Z, Zhang N, et al. Autocrine STIP1 signaling promotes tumor growth and is associated with disease outcome in hepatocellular carcinoma. Biochem Biophys Res Commun. 2017;493(1):365-72.
42. Lin L, Wen J, Lin B, Xia E, Zheng C, Ye L, et al. Stress-induced phosphoprotein 1 facilitates breast cancer cell progression and indicates poor prognosis for breast cancer patients. Hum Cell. 2021;34(3):901-17.
43. Wang JH, Gong C, Guo FJ, Zhou X, Zhang MS, Qiu H, et al. Knockdown of STIP1 inhibits the invasion of CD133-positive cancer stem-like cells of the osteosarcoma MG63 cell line via the PI3K/Akt and ERK1/2 pathways. Int J Mol Med. 2020;46(6):2251-9.
44. Luo J, Feng ZS, Tang JX. The essential role of CCT2 in the regulation of aggrephagy. Front Aging Neurosci. 2024;16:1491001.
45. Chen F, Wang T, Feng C, Lin G, Zhu Y, Wu G, et al. Proteome Differences in Placenta and Endometrium between Normal and Intrauterine Growth Restricted Pig Fetuses. PLOS ONE. 2015;10(11):e0142396.
46. Liu Q, Qi Y, Kong X, Wang X, Zhang W, Zhai J, et al. Molecular and Clinical Characterization of CCT2 Expression and Prognosis via Large-Scale Transcriptome Profile of Breast Cancer. Front Oncol. 2021;11:614497.
47. Park SH, Jeong S, Kim BR, Jeong YA, Kim JL, Na YJ, et al. Activating CCT2 triggers Gli-1 activation during hypoxic condition in colorectal cancer. Oncogene. 2020;39(1):136-50.
48. Kay HH, Zhu S, Tsoi S. Hypoxia and lactate production in trophoblast cells. Placenta. 2007;28(8-9):854-60.
49. Ma LN, Huang XB, Muyayalo KP, Mor G, Liao AH. Lactic Acid: A Novel Signaling Molecule in Early Pregnancy? Front Immunol. 2020;11:279.
50. Urbańska K, Orzechowski A. Unappreciated Role of LDHA and LDHB to Control Apoptosis and Autophagy in Tumor Cells. Int J Mol Sci. 2019;20(9):2085.
51. McCleland ML, Adler AS, Shang Y, Hunsaker T, Truong T, Peterson D, et al. An integrated genomic screen identifies LDHB as an essential gene for triple-negative breast cancer. Cancer Res. 2012;72(22):5812-23.
52. Turhan U, Tatar B. The association between increased maternal PARK7 (DJ-1) levels and the occurrence of preterm premature rupture of membranes - A randomized prospective study. Turk J Obstet Gynecol. 2021;18(4):279-84.
53. Jin W. Novel Insights into PARK7 (DJ-1), a Potential Anti-Cancer Therapeutic Target, and Implications for Cancer Progression. J Clin Med. 2020;9(5):1256.
54. Zhu GM, Chen SQ, Jiang QG, Cao Y, Guo Y, Ye LQ. MiR-216b inhibits gastric cancer proliferation and migration by targeting PARK7. Indian J Pathol Microbiol. 2021;64(1):52-7.
55. Scumaci D, Olivo E, Fiumara CV, La Chimia M, De Angelis MT, Mauro S, et al. DJ-1 Proteoforms in Breast Cancer Cells: The Escape of Metabolic Epigenetic Misregulation. Cells. 2020;9(9):1968.
56. Ismail IA, Kang HS, Lee HJ, Kim JK, Hong SH. DJ-1 upregulates breast cancer cell invasion by repressing KLF17 expression. Br J Cancer. 2014;110(5):1298-306.
57. Ismail T, Kim Y, Lee H, Lee DS, Lee HS. Interplay Between Mitochondrial Peroxiredoxins and ROS in Cancer Development and Progression. Int J Mol Sci. 2019;20(18).
58. Nicolussi A, D'Inzeo S, Capalbo C, Giannini G, Coppa A. The role of peroxiredoxins in cancer. Mol Clin Oncol. 2017;6(2):139-53.
59. Chang XZ, Li DQ, Hou YF, Wu J, Lu JS, Di GH, et al. Identification of the functional role of peroxiredoxin 6 in the progression of breast cancer. Breast Cancer Res. 2007;9(6):R76.
60. Garbi N, Tanaka S, Momburg F, Hämmerling GJ. Impaired assembly of the major histocompatibility complex class I peptide-loading complex in mice deficient in the oxidoreductase ERp57. Nat Immunol. 2006;7(1):93-102.
61. Wang S, He Z, Wang X, Li H, Liu XS. Antigen presentation and tumor immunogenicity in cancer immunotherapy response prediction. Elife. 2019;8:e49020.
62. Bhattacharya K, Weidenauer L, Luengo TM, Pieters EC, Echeverría PC, Bernasconi L, et al. The Hsp70-Hsp90 co-chaperone Hop/Stip1 shifts the proteostatic balance from folding towards degradation. Nat Commun. 2020;11(1):5975.
63. Bohonowych JE, Gopal U, Isaacs JS. Hsp90 as a gatekeeper of tumor angiogenesis: clinical promise and potential pitfalls. J Oncol. 2010;2010:412985.

64. Chowdhury I, Mo Y, Gao L, Kazi A, Fisher AB, Feinstein SI. Oxidant stress stimulates expression of the human peroxiredoxin 6 gene by a transcriptional mechanism involving an antioxidant response element. Free Radic Biol Med. 2009;46(2):146-53.
65. Li HX, Sun XY, Yang SM, Wang Q, Wang ZY. Peroxiredoxin 1 promoted tumor metastasis and angiogenesis in colorectal cancer. Pathol Res Pract. 2018;214(5):655-60.
66. Wang ZH, Peng WB, Zhang P, Yang XP, Zhou Q. Lactate in the tumour microenvironment: From immune modulation to therapy. EBioMedicine. 2021;73:103627.
67. Assaye MA, Gizaw ST. Chaperone-Mediated Autophagy and Its Implications for Neurodegeneration and Cancer. Int J Gen Med. 2022;15:5635-49.
68. Lee DH, Kim D, Kim ST, Jeong S, Kim JL, Shim SM, et al. PARK7 modulates autophagic proteolysis through binding to the N-terminally arginylated form of the molecular chaperone HSPA5. Autophagy. 2018;14(11):1870-85.
69. Henderson MC, Silver M, Tran Q, Letsios EE, Mulpuri R, Reese DE, et al. A noninvasive blood-based combinatorial proteomic biomarker assay to detect breast cancer in women over age 50 with BI-RADS 3, 4, or 5 assessment. Clin Cancer Res. 2019;25(1):142-9.
70. Chapman C, Murray A, Chakrabarti J, Thorpe A, Woolston C, Sahin U, et al. Autoantibodies in breast cancer: their use as an aid to early diagnosis. Annals of Oncology. 2007;18(5):868-73.
71. Liu W, De La Torre IG, Gutiérrez-Rivera MC, Wang B, Liu Y, Dai L, et al. Detection of autoantibodies to multiple tumor-associated antigens (TAAs) in the immunodiagnosis of breast cancer. Tumour Biol. 2015;36(2):1307-12.
72. Desmetz C, Bascoul-Mollevi C, Rochaix P, Lamy PJ, Kramar A, Rouanet P, et al. Identification of a new panel of serum autoantibodies associated with the presence of in situ carcinoma of the breast in younger women. Clin Cancer Res. 2009;15(14):4733-41.
73. Ye H, Sun C, Ren P, Dai L, Peng B, Wang K, et al. Mini-array of multiple tumor-associated antigens (TAAs) in the immunodiagnosis of breast cancer. Oncol Lett. 2013;5(2):663-8.
74. Qiu C, Wang B, Wang P, Wang X, Ma Y, Dai L, et al. Identification of novel autoantibody signatures and evaluation of a panel of autoantibodies in breast cancer. Cancer Sci. 2021;112(8):3388-400.
75. Tainsky MA, Tabernero MD, Lv L-L, Anderson KS. Autoantibody profiles as biomarkers of breast cancer. Cancer Biomarkers. 2009;6(5-6):247-56.
76. Lastwika KJ, Lampe PD. Breaking tolerance: autoantibodies can target protein posttranslational modifications. Curr Opin Biotechnol. 2024;85:103056.
77. Geffen Y, Anand S, Akiyama Y, Yaron TM, Song Y, Johnson JL, et al. Pan-cancer analysis of post-translational modifications reveals shared patterns of protein regulation. Cell. 2023;186(18):3945-67.e26.

Figures

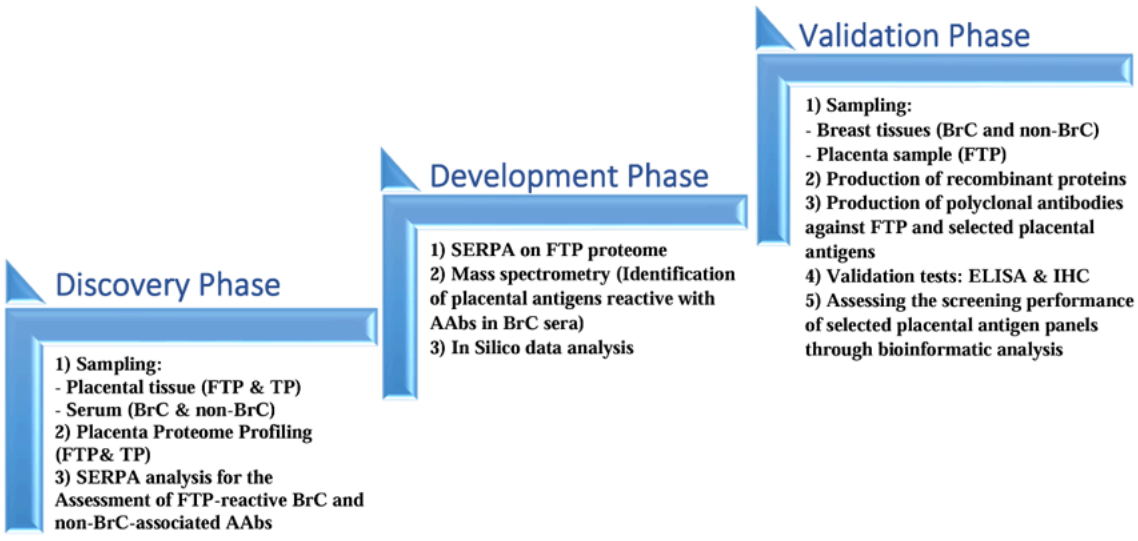


Figure 1

Flowchart of study design. This diagram illustrates the process used to identify and validate autoantibodies targeting placental proteins in breast cancer patients' sera. FTP: First-trimester placenta, TP: Term placenta, BrC: Breast cancer, AAb: Autoantibody, SERPA: Serological proteome analysis.

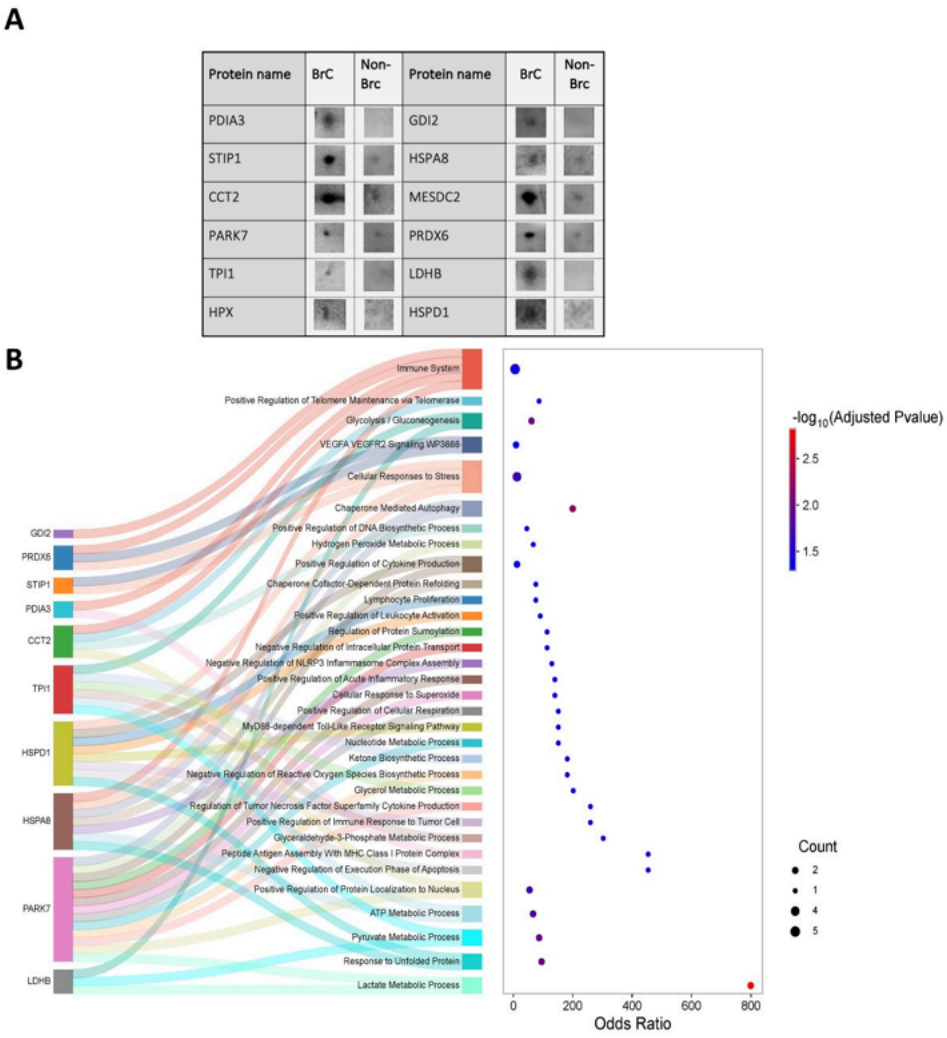


Figure 2

Selected placental proteins reactive with breast cancer-associated autoantibodies. Based on mass report and review of SERPA results, 12 proteins were selected for validation phase. Fig.2a shows the close-up sections of SERPA reactivity of these proteins in BrC or non-BrC serum samples. Fig.2b depicts a Sankey dot plot to highlight the connections between these proteins and the significantly enriched GO terms. The analysis identified 33 GO terms with significant enrichment, most of which fell under the Biological Process category. Notably, a large proportion of the proteins were involved in immune system processes and cellular response to stress.

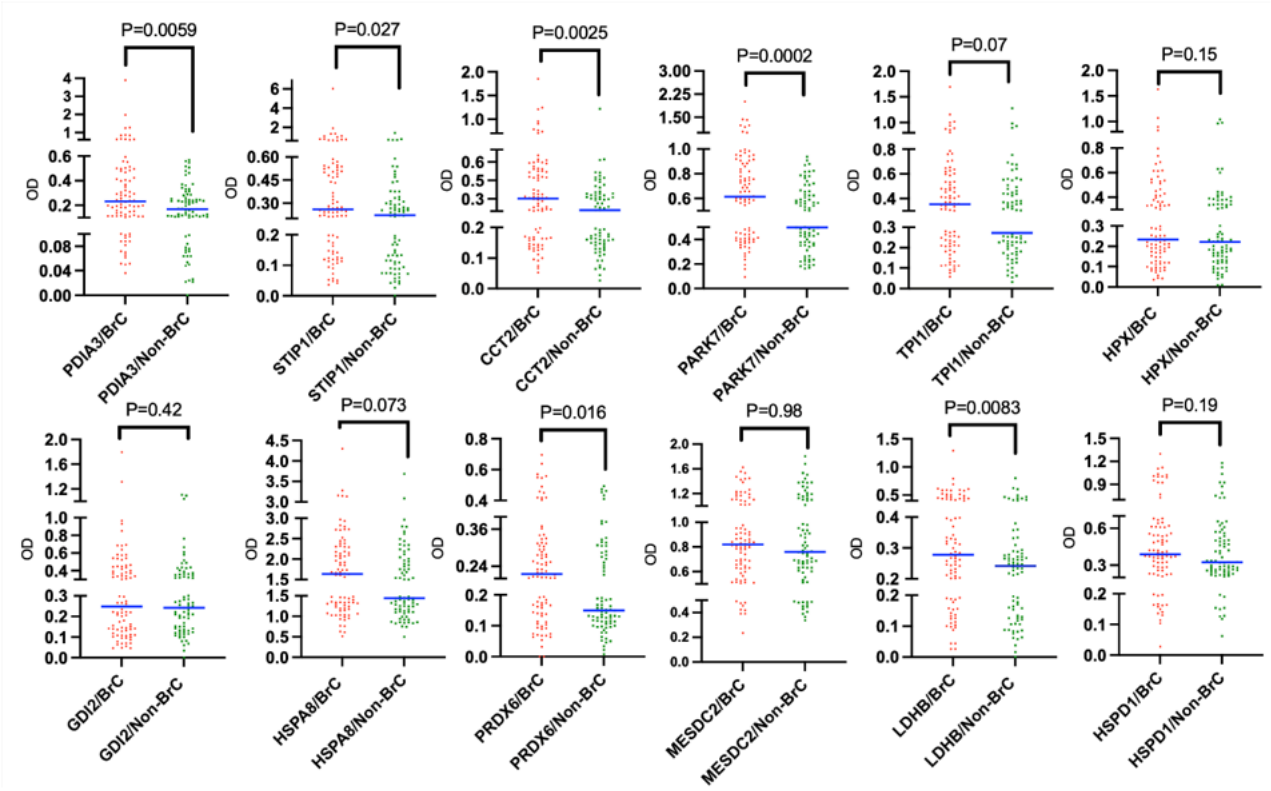


Figure 3

Immune reactivity of sera from breast cancer patients with selected placental proteins. Selected placental proteins were used as coating antigen in ELISA, and immune reactivity of IgG isotype of sera from 86 breast cancer and 86 non-breast cancer women was separately examined. BrC: Breast cancer.

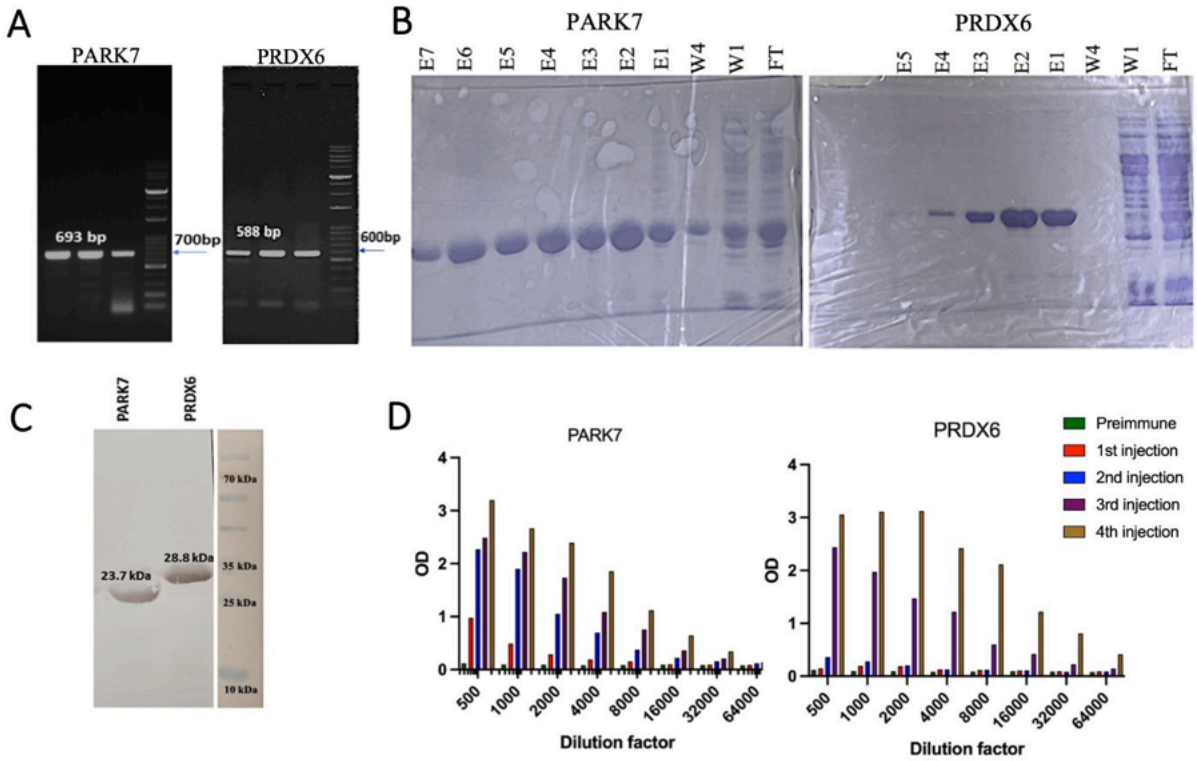


Figure 4

Generation and analysis of recombinant PARK7/PRDX6 and their specific antibodies. Successful gene cloning was verified by colony PCR, which detected the 693bp PRDX6 and 588bp PARK7 amplicons (Fig.4A). The recombinant proteins were subsequently purified via Ni-affinity chromatography, and their purity and identity were confirmed by SDS-PAGE (Fig.4B) and Western blotting using an anti-His tag antibody (Fig.4C). Furthermore, polyclonal antibodies raised against the recombinant PARK7 and PRDX6 proteins demonstrated specific binding to their respective antigens in an ELISA (Fig.4D). FT: Flowthrough, W: Wash, E: Elution.

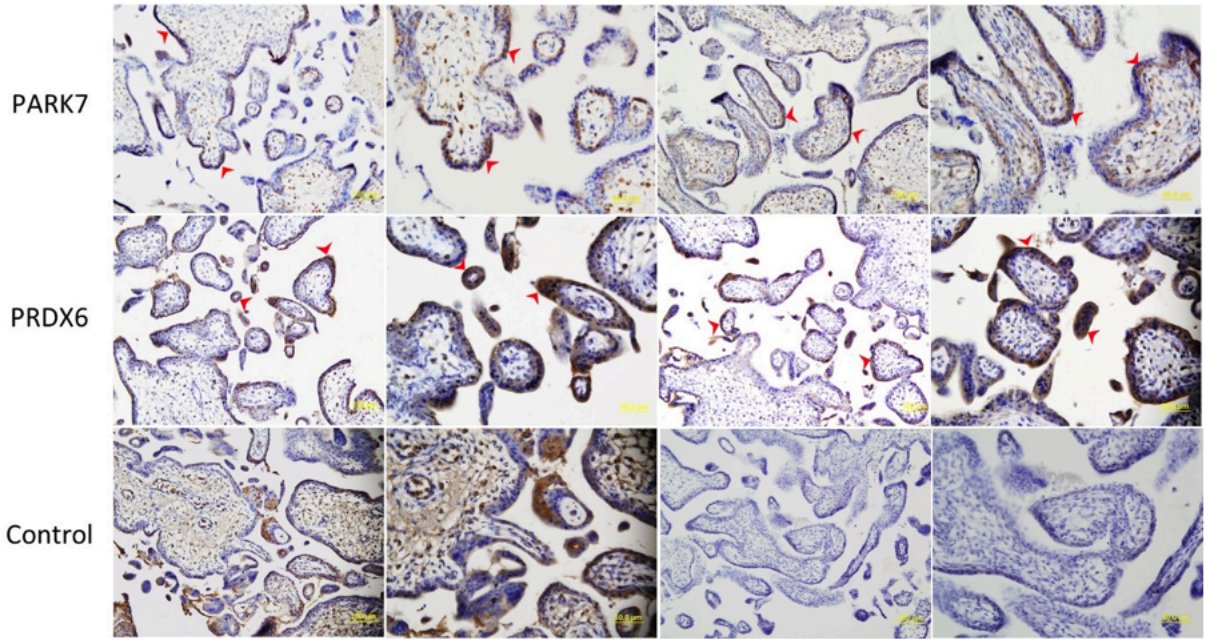


Figure 5

Immunohistichemical localization of PARK7 and PRDX6 in placental tissues. To locate the placental proteins targeted by breast cancer autoantibodies, we performed immunohistochemistry on FTP tissue using antibodies for PARK7 and PRDX6. PARK7 was primarily found in the nucleus and cytoplasm of cytotrophoblasts, with little presence in syncytiotrophoblasts. In contrast, PRDX6 was mainly located in the cytoplasm of syncytiotrophoblasts. Red arrowheads indicate positive staining. Controls included serum from a rabbit immunized with placental lysate (positive control) and pre-immune rabbit serum (negative control).

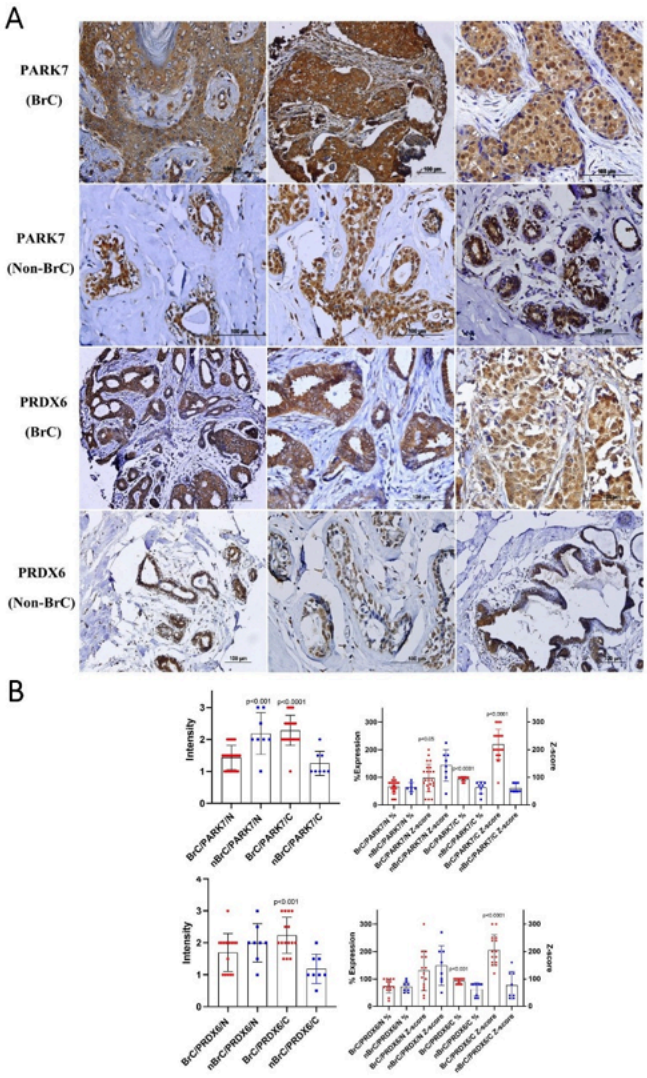


Figure 6

The expression pattern of PARK7 and PRDX6 in breast cancer tissues. The subcellular localization of PRDX6 and PARK7 was assessed in normal breast tissue and invasive ductal carcinoma (IDC). Glandular epithelial cells in normal tissue displayed predominantly nuclear staining for both proteins, with faint cytoplasmic presence. In IDC tissues, this pattern was reversed, with a marked shift to cytoplasmic expression and a concurrent reduction in nuclear reactivity (Fig. 6a). Quantitative evaluation revealed that breast cancer tissues had significantly lower nuclear staining intensity and Z-scores for PARK7, but significantly higher cytoplasmic intensity, staining percentage, and Z-scores. PRDX6 expression followed a comparable trend, with a significant redistribution from the nucleus to the cytoplasm in malignant tissues (Fig. 6b). All staining was specific, as negative controls showed no reactivity.

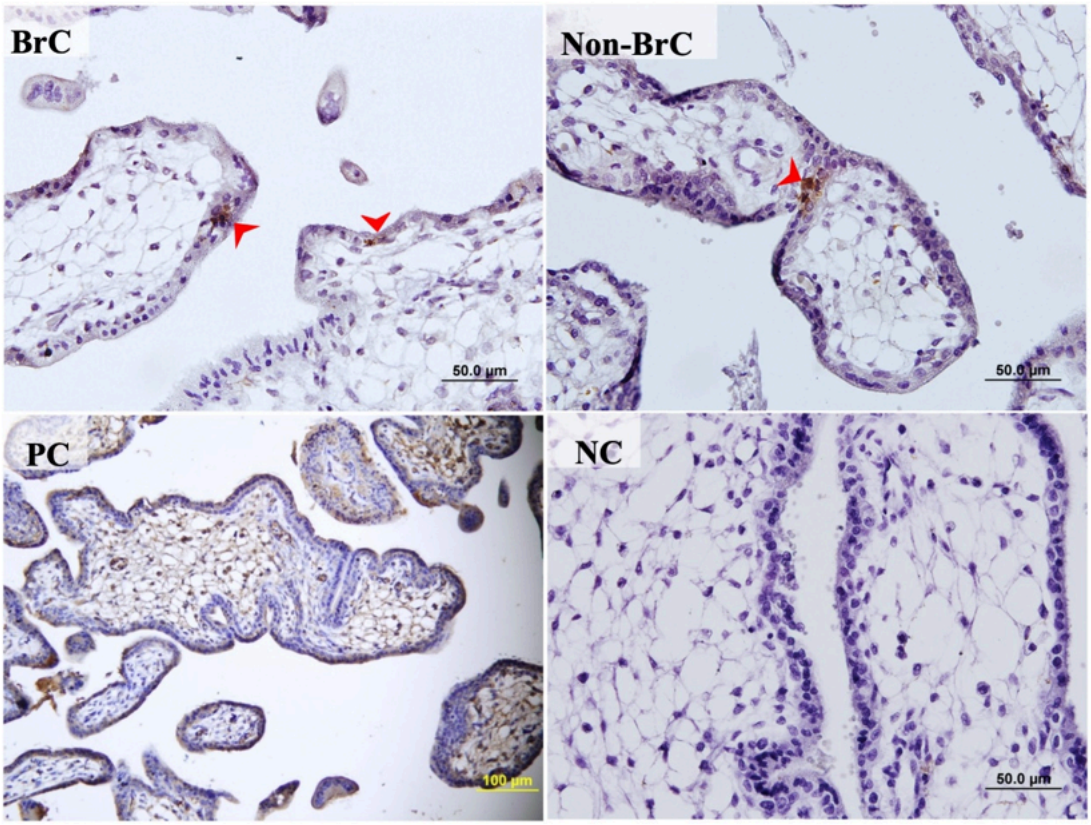


Figure 7

Reactivity of breast cancer associated autoantibodies with human placenta. We performed immunohistochemistry on FTP using serum from breast cancer (BrC) patients and healthy (non-BrC) individuals. The BrC serum showed a highly specific staining pattern, binding to a rare subset of cells in the cytotrophoblast layer and to syncytial nuclear aggregates. This binding was primarily located in the nucleus and cytoplasm of these cells. Non-BrC samples showed fewer reactive cells.

Supplementary Files

This is a list of supplementary files associated with this preprint. Click to download.

- JournalofTranslationalMedicine.pdf
- SupplementaryFiguresandLegends.docx